THE EUROPEAN
PHYSICAL JOURNAL C

Selected strong decays of pentaquark State $P_c(4312)$ in a chiral constituent quark model

Yubing Dong[1,2,3,a], **Pengnian Shen**[1,2,4,b], **Fei Huang**[5,c], **Zongye Zhang**[1,2,3,d]

[1] Institute of High Energy Physics, Chinese Academy of Sciences, Beijing 100049, China
[2] Theoretical Physics Center for Science Facilities (TPCSF), CAS, Beijing 100049, China
[3] School of Physical Sciences, University of Chinese Academy of Sciences, Beijing 101408, China
[4] College of Physics and Technology, Guangxi Normal University, Guilin 541004, China
[5] School of Nuclear Science and Technology, University of Chinese Academy of Sciences, Beijing 101408, China

Abstract The newly confirmed pentaquark state $P_c(4312)$ has been treated as a weakly bound ($\Sigma_c \bar{D}$) state by a well-established chiral constituent quark model and by a dynamical calculation on quark degrees of freedom where the quark exchange effect is accounted for. The obtained mass 4308 MeV agrees with data. In this work, the selected strong decays of the $P_c(4312)$ state are studied with the obtained wave function. It is shown that the width of the $\Lambda_c \bar{D}^*$ decay is overwhelmed and the branching ratios of the $p \eta_c$ and $p J/\psi$ decays are both less than 1 percentage.

1 Introduction

Since the discovery of $X(3872)$ in 2003, the study of XYZ particles has been a hot topic in hadron physics. On the one hand, many theoretical studies have been carried out in order to understand the peculiar characteristics of these exotic particles, such as their very narrow widths and the fact that they are very close to the open thresholds. The molecular scenario, tetraquark picture, kinematics triangle singularity, and cusp are the most popular interpretations [1–10]. On the other hand, many experiments in BEPCII, BELLE, Jefferson Lab., LHCb, etc. have also been performed for hunting these exotics [11–13].

In 2015, in addition to four-quark XYZ meson sectors, LHCb first announced that two pentaquark states $P_c(4310)$ and $P_c(4450)$ were discovered in the decay of $\Lambda_b \to J/\psi p K$ in Run I [14]. Moreover, they updated their find-

ing in the year of 2019 [15] by careful analyzing the data set including those collected in Run II. Three, instead of two, pentaquark states were confirmed. Their masses and widths are [15]

$$(M, \ \Gamma)_{P_c(4312)} = \left(4311.9 \pm 0.7^{+6.8}_{-0.6}, \ \ 9.8 \pm 2.7^{+3.5}_{-4.5}\right) \text{MeV},$$

$$(M, \ \Gamma)_{P_c(4440)} = \left(4440.3 \pm 1.3^{+4.1}_{-4.7}, \ \ 20.6 \pm 4.9^{+8.7}_{-10.1}\right) \text{MeV},$$

$$(M, \ \Gamma)_{P_c(4457)} = \left(4457.3 \pm 0.6^{+4.1}_{-1.7}, \ \ 6.4 \pm 2.0^{+5.7}_{-1.9}\right) \text{MeV}.$$

The significance of the new $P_c(4312)$ state is 7.3σ, while such a quantity for $P_c(4440)$ and $P_c(4457)$ is 5.7σ.

After P_c states were firstly discovered in 2015, many theoretical investigations have been devoted to the investigation of the properties of the two exotic baryon states of $P_c(4310)$ and $P_c(4450)$. In particular, the latest experimental analysis has stimulated a great interest in further understanding of these three pentaquark states [16–26]. Various models, such as meson-baryon molecular scenario, compact five quark states, cusp effect as well as kinematical triangle singularity, etc. have been proposed to accommodate their structures [27–33]. In fact, even before the LHCb's discovery, theorists have already performed some model calculations, which can correctly predict the existence of the bound state of the baryon-meson system with heavy flavor in both quark and hadron degrees of freedom [34–37]. The chiral constituent quark model is one of them [36].

The chiral constituent quark model is a successful model which has been frequently used to calculate the properties of single hadrons and multi-quark states, especially, the states which may have cluster structures, in a dynamical and systematical way. As its achievements, the model calculation can well-reproduce the natures of a six light-quark system with cluster structures, like the phase shifts of the

[a] e-mail: dongyb@ihep.ac.cn (corresponding author)

[b] e-mail: shenpn@ihep.ac.cn

[c] e-mail: huangfei@ucas.ac.cn

[d] e-mail: zhangzy@ihep.ac.cn

nucleon-nucleon scattering, the binding energy, wave function with S-D admixture and form factors of the deuteron, the cross sections of the hyperon-nucleon interactions, and etc., with the same set of model parameters which was fixed before hand by the data of the nucleon-nucleon scattering and other processes. Meanwhile, it can give a reasonable spectrum of low-lying baryon resonances as well. More than twenty years ago, this model has been adopted to the study the existence of dibaryon resonance [38–42], especially the $\Delta\Delta$ resonance (later called $d^*(2380)$ [43]) which eventually was observed by WASA@COSY collaboration in 2014 [44–47] (see the review of Ref. [48]). Recently, the extracted wave function of $d^*(2380)$ was further employed to calculate the strong decays of $d^*(2380)$ [49–53], the electromagnetic form factors [54,55], and the deuteron to $d^*(2380)$ transition form factors [56]. It is shown that the results with the quark exchange effect on the quark degrees of freedom fairly-well agree with the experimental data, and therefore one can interpret $d^*(2380)$ as a compact hexaquark system where the effects of the hidden-color component and the quark exchange play important roles in producing its narrow widths [43,48,53,57–59].

In analogy to the dibaryon $d^*(2380)$ case, this kind of cluster model calculation was also performed for the meson-baryon system $(\bar{D}\Sigma_c)$ in 2011 [36] before the discovery of LHCb. Based on the dynamics of the chiral constituent quark model, we found a weakly bound state with the mass of $4279 - 4312$ MeV. Clearly, this state just corresponds to the observed $P_c(4312)$ resonance with the negative parity. It reflects once more that this kind of cluster model calculation on the quark degrees of freedom is suitable for unveiling the nature of the hadron. Especially, when the employed chiral constituent quark model can well-reproduce the existing data, the model has predictive power. The distinguishing feature of such a treatment, which cannot be involved in the study on the hadron degrees of freedom, is that the quark exchange effect will be explicitly taken into account in the calculation. Furthermore, because all the model parameters are pre-determined in previous calculations for the better explanations of the existing data, no any additional phenomenological form factors or phenomenological vertices among P_c, $\bar{D}$, and Σ_c are needed by hand. Therefore, the obtained P_c state is more reliable and less ambiguity.

In this work, we will employ the $P_c(4312)$ wave function obtained in our previous calculation, where the $P_c(4312)$ state is a weakly bound $\bar{D}\Sigma_c$ state with a mass of around 4308 MeV, to study the selected strong decays of $P_c(4312)$. Section 2 gives a brief introduction of the dynamics of the chiral constituent quark model. Section 3 devotes to some selected strong decay processes of $P_c(4312)$, $P_c(4312) \rightarrow J/\psi\, p$, $P_c(4312) \rightarrow \eta_c\, P$ as well as $P_c(4312) \rightarrow \bar{D}^*\Lambda_c$. Finally, we provide a short summary in Sect. 4.

2 Structure and wave function of $P_c(4312)$ in the extended chiral constituent quark model

In our previous study of the pentaquark state with heavy flavor, a system of an open-charm meson and an open-charm baryon is considered, and a so-called extended chiral SU(3) constituent quark model (ECCQM) that provides the basic effective quark-quark interactions caused by the exchanges of the chiral fields, including pseudo-scalar, scalar and vector mesons, and of one gluon, as well as the quark confinement, were employed in a dynamical Resonant group method calculations on the quark degrees of freedom. Specifically, in this theoretical model, the Hamiltonian for a 5-quark system is written as

$$H = \sum_{i=1}^{5} T_i - T_G + \sum_{j>i=1}^{5} \left(V_{ij}^{OGE} + V_{ij}^{Conf.} + V_{ij}^{chv.} \right),$$

(1)

with T_i being the kinetic energy operator for the $i-th$ quark and T_G the kinetic energy operator for the center of mass (CM) motion, V_{ij}^{OGE}, $V_{ij}^{Conf.}$, and $V_{ij}^{chv.}$ denoting the one-gluon exchange potential, confinement potential, and the quark-quark potential operators caused by the chiral fields between the $i-th$ and $j-th$ quarks, respectively [43]. The latter one can be abbreviated as

$$V_{ij}^{chv.} = \sum_{a=0}^{8} V_{ij}^{\sigma_a} + \sum_{a=0}^{8} V_{ij}^{\pi_a} + \sum_{a=0}^{8} V_{ij}^{\rho_a},$$

(2)

and the explicit forms of these effective potentials can be found in our previous papers [43,58,59]. In order to make the model predictive, the determination of parameters must ensure that as many existing data as possible including the stability conditions, the masses of the ground state baryons, the static properties of baryons, the binding energy, root-mean-square radius (RMS), $S-$ and $D-$ wave admixture in the wave function of deuteron, the phase shifts of the N-N scattering and the cross sections of the N-hyperon (N-Y) interactions, and even the binding behavior of H-particle and the property of $d^*(2380)$, can all be well-reproduced. The detailed procedure for the determination of model parameters can also be found in our previous papers [43,58,59].

The wave function of $P_c(4312)$ obtained in our previous calculation [36] can be expressed as

$$\Psi_{5q,total}^{LSTC} = \sum_i c_i \Psi^{LSTC}(\vec{S}_i)$$

(3)

with the superscripts L, S, T, and C denoting the orbital, spin, isospin, and color, and

$$\Psi^{LSTC}(\vec{S}_i)$$
$$= \mathcal{A}\left[\phi_A(\vec{\xi}_1, \vec{\xi}_2)\phi_B(\vec{\xi}_3)\chi^L(\vec{r}_{AB} - \vec{S}_i)\Psi_A^{(STC)_A}\Psi_B^{(STC)_B}\right]$$

$$= \mathcal{A} \Big[\Pi_{k=1}^{3} \psi_A \Big(\vec{r}_k, \frac{\mu_{AB}}{M_A} \vec{S}_i \Big)$$

$$\otimes \Pi_{l=4}^{5} \psi_B \Big(\vec{r}_l, -\frac{\mu_{AB}}{M_B} \vec{S}_i \Big) \Psi_A^{(STC)_A} \Psi_B^{(STC)_B} \Big], \qquad (4)$$

where the wave function of the CM motion is omitted in the first row, because we are working in the CM system (the unitary transformation between two sets of coordinates in the first and second rows, respectively, can be found in Appendix). In the equality above, $\mathcal{A}$ denotes the anti-symmetrization operator which can be written as

$$\mathcal{A} = \big(1 - \hat{P}_{14}^{OSFC} - \hat{P}_{24}^{OSFC} - \hat{P}_{34}^{OSFC} \big), \qquad (5)$$

where $\hat{P}_{ij}^{OSFC}$ is an exchange operator which exchanges the i-th quark in cluster A and the j-th quark in cluster B in the orbital, spin, flavor and color spaces, and the first and other three terms on the right hand side of Eq. (5) are the direct term and exchange terms in order. $\Psi_{A,B}^{(STC)_{A,B}}$ is the wave function in the spin-flavor-color space for cluster A or B, and consequently, the color wave function of the direct term of P_c can be expressed as

$$\Psi_{5q}^{C} = \frac{1}{\sqrt{6}} \sum_{ijk} \epsilon_{ijk} q_i^{(1)} q_j^{(2)} q_k^{(3)} \otimes \frac{1}{\sqrt{3}} \delta_{kl} q_k^{(4)} \bar{q}_l^{(5)}, \qquad (6)$$

and the spin-flavor wave function of the direct term of P_c can be written as

$$\Psi_{5q}^{(SF)} = \frac{1}{\sqrt{2}} \Big[\chi_\rho \xi_\rho + \chi_\lambda \xi_\lambda \Big]_{(SF)_{\Sigma_c}}^{(123)} \otimes \Big(q^{(4)} \bar{q}^{(5)} \Big)_{(SF)_{\bar{D}}}, \quad (7)$$

with $\xi_{\rho,\lambda}$ (or $\chi_{\rho,\lambda}$) being the isospin (or spin) wave function with the mixed-antisymmetry ρ and mixed-symmetry λ, respectively, and the number in parentheses in the superscript indicating the label of the quark. The detailed forms of $\xi_{\rho,\lambda}$ (or $\chi_{\rho,\lambda}$) can be found in the standard text book, for instance Ref. [60]. $\phi_A(\vec{\xi}_1, \vec{\xi}_2)$ for quarks labeled 1,2,3 and $\phi_B(\vec{\xi}_3)$ for quarks labeled 4,5 represent, respectively, the internal wave functions of the baryon and meson clusters in the coordinate space:

$$\phi_A(\vec{\xi}_1, \vec{\xi}_2)$$

$$= \Big(\frac{\omega}{\pi} \frac{m_1 m_2}{m_{12}} \Big)^{3/4} \Big(\frac{\omega}{\pi} \frac{m_{12} m_3}{m_{123}} \Big)^{3/4}$$

$$\exp \Big[-\frac{\omega}{2} \Big(\frac{m_1 m_2}{m_{12}} \vec{\xi}_1^2 + \frac{m_{12} m_3}{m_{123}} \vec{\xi}_2^2 \Big) \Big]$$

$$= \Big(\frac{\omega}{\pi} \mu_{12} \Big)^{3/4} \Big(\frac{\omega}{\pi} \mu_{(12),3} \Big)^{3/4}$$

$$\exp \Big[-\frac{\omega}{2} \Big(\mu_{12} \vec{\xi}_1^2 + \mu_{(12),3} \vec{\xi}_2^2 \Big) \Big], \qquad (8)$$

with $m_{12} = m_1 + m_2$, $\mu_{(12,3)} = \frac{m_{12} m_3}{m_{12} + m_3}$, $\vec{\xi}_1 = \vec{r}_2 - \vec{r}_1$, $\vec{\xi}_2 = \vec{r}_3 - \frac{m_1 \vec{r}_1 + m_2 \vec{r}_2}{m_1 + m_2}$, and

$$\phi_B(\vec{\xi}_3) = \Big(\frac{\omega}{\pi} \frac{m_4 m_5}{m_{45}} \Big)^{3/4} \exp \Big[-\frac{\omega}{2} \frac{m_4 m_5}{m_{45}} \vec{\xi}_3^2 \Big]$$

$$= \Big(\frac{\omega}{\pi} \mu_{45} \Big)^{3/4} \exp \Big[-\frac{\omega}{2} \mu_{45} \vec{\xi}_3^2 \Big], \qquad (9)$$

with $\vec{\xi}_3 = \vec{r}_5 - \vec{r}_4$. Functions

$$\chi^L(\hat{r}_{AB} - \vec{S}_i) = \Big(\frac{\omega}{\pi} \mu_{AB} \Big)^{3/4} \exp \Big[-\frac{\omega}{2} \mu_{AB} \big(\hat{r}_{AB} - \vec{S}_i \big)^2 \Big], \qquad (10)$$

with $\mu_{AB} = \frac{(m_1 + m_2 + m_3)(m_4 + m_5)}{m_1 + m_2 + m_3 + m_4 + m_5}$, form a set of basis functions peaked locally at $\vec{S}_i$, which span a domain in the coordinate space for expanding the unknown relative motion wave function between two clusters, and c_i are expansion coefficients which are determined by solving the bound state RGM equation [58,59]:

$$\langle \delta \Psi_{5q} | H - E | \Psi_{5q} \rangle = 0 \qquad (11)$$

for P_c.

In the practical calculation, we only consider the single configuration $\bar{D}\Sigma_c$. This is because that the effect of the channel mixing from other configurations, like $\bar{D}\Lambda_c$, hidden-color state $|c_8 c_8 >$, and etc. is negligible due to the large threshold difference (in fact, our previous calculation confirmed such a statement). Now, if we consider the spin-parity of this pentaquark state is $1/2^-$, the resultant mass of the state is around 4308 MeV, which is very close to the experimental data $4311.9 \pm 0.7^{+6.8}_{-0.6}$. Meanwhile, we also obtain the wave function of this P_c state.

3 Selected strong decays of $P_c(4312)$

Nowadays, confirming the structure of P_c is an urgent task for the research on the existence of pentaquark states. One of the most effective ways is to theoretically study its decay modes and corresponding partial decay widths, and to provide a reference for further verification by experiments. To this end, we select some dominant decay channels, for instance the $J/\psi + p$, $\eta_c + p$, $\bar{D}^* + \Lambda_c$, $\bar{D} + \Lambda_c$ channels, to study. Since we assume that the initial state has a $\Sigma_c + \bar{D}$ structure, the decayed particles are different from the clusters in the initial state. Therefore, there must be quark re-combination or re-arrangement in the decay processes. In fact, that kind of process has been discussed and considered in the meson-meson scattering [61–63], as well as the $N\bar{N}$ annihilation processes [64–66] in the past. We believe that such effect will also play a role in the decay of P_c. Now, in terms of the obtained wave function of P_c in the bound state calculation, we include this effect in the $P_c(4312)$ decays.
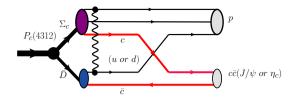
Fig. 1 Schematic diagram for the hidden charm decay $P_c(\Sigma_c + \bar{D}) \to p + J/\psi(\eta_c)$ with the quark re-arrangement. The wiggle line stands for the interaction between two quarks in the meson and baryon clusters, respectively. The thin-black and red-thick lines represent the light and heavy quarks, respectively

Then, the decay width of the $P_c(4312)$ state to two hadrons, for instance, J/ψ and p, in our non-relativistic chiral constituent quark model, can be written as

$$\Gamma = \frac{1}{2S_{P_c} + 1} \int (2\pi)\delta\Big(M_{P_c} - E_{J/\psi}(k) - E_p(k)\Big)d^3k\overline{|\mathcal{M}_{fi}(k)|^2},$$
(12)

where $\vec{k}$ denotes the three-momentum of the relative momentum between two outgoing hadrons, $c\bar{c}$ (can be either J/ψ or η_c) and p with $\vec{k} = -\frac{M_{c\bar{c}}}{M_p+M_{c\bar{c}}}\vec{P}_p + \frac{M_p}{M_p+M_{c\bar{c}}}\vec{P}_{c\bar{c}}$, where $\vec{P}_{c\bar{c}}$ and $\vec{P}_p$ are the momenta of the outgoing $c\bar{c}$ and proton, respectively. The magnitude of the relative momentum k can be expressed as

$$k = \lambda^{1/2}\big(M_{P_c}^2, M_{J/\psi}^2, M_p^2\big)\Big/(2M_{P_c}),$$
(13)

with the Källen function

$$\lambda(x, y, z) = x^2 + y^2 + z^2 - 2xy - 2xz - 2yz.$$
(14)

3.1 Hidden charm decays

Because the P_c states were discovered in the $\Lambda_b^0 \to J/\psi p K^-$ process at LHCb, it is necessary to study the hidden-charm decay of the P_c state. For the decay mode $P_c \to (c\bar{c})p$ (where $c\bar{c} = J/\psi$ or η_c) we consider the re-arrangement of the heavy quark (the 3-rd quark in the initial Σ_c-cluster) and the light quark (the 4-th quark in the initial $\bar{D}$-cluster) shown in Fig. 1.

Similar to Eq. (7), the spin-isospin wave function of the final p and J/ψ states is given by

$$\Psi_{5q}^{(SF)} = \frac{1}{\sqrt{2}}\Big[\chi_\rho\xi_\rho + \chi_\lambda\xi_\lambda\Big]_{(SF)_p}^{(124)} \otimes \Big(q^{(3)}\bar{q}^{(5)}\Big)_{(SF)_{J/\psi}},$$
(15)

where the superscript (124) indicates that quarks in p are labeled by 1, 2, and 4, and (3) and (5) denotes that quarks in J/ψ are marked by 3 and 5, respectively. The detailed forms of $\xi_{\rho,\lambda}$ (or $\chi_{\rho,\lambda}$) can also be found in Ref. [60].

The orbital wave function of the final state after considering the quark re-arrangement can be expressed as

$$\Psi_f = \phi_{A'}(\xi_1', \xi_2')\phi_{B'}(\xi_3')\frac{\exp(i\vec{k} \cdot \vec{r}_{A'B'}')}{\sqrt{V}}\frac{\exp(i\vec{\mathcal{P}} \cdot \vec{R}_{A'B'}')}{\sqrt{V}}$$
(16)

with

$$\phi_{A'}(\vec{\xi}_1', \vec{\xi}_2')$$
$$= \Big(\frac{1}{b_{p_1}^2\pi}\Big)^{3/4}\Big(\frac{1}{b_{p_2}^2\pi}\Big)^{3/4}$$
$$\exp\Big[-\frac{1}{2b_{p_1}^2}\vec{\xi}_1'^2 - \frac{1}{2b_{p_2}^2}\vec{\xi}_2'^2\Big]$$
$$= \Big(\frac{1}{b_{p_1}^2\pi}\Big)^{3/4}\Big(\frac{1}{b_{p_2}^2\pi}\Big)^{3/4}$$
$$\exp\Big[-\frac{1}{2b_{p_1}^2}\vec{\xi}_1^2 - \frac{1}{2b_{p_2}^2}\Big(\vec{r}_{AB} - \frac{m_c}{m_{123}}\vec{\xi}_2 + \frac{m_c}{m_{45}}\vec{\xi}_3\Big)^2\Big],$$
(17)

and

$$\phi_{B'}(\vec{\xi}_3') = \Big(\frac{1}{b_{c\bar{c}}^2\pi}\Big)^{3/4}\exp\Big[-\frac{\vec{\xi}_3'^2}{2b_{c\bar{c}}^2}\Big]$$
$$= \Big(\frac{1}{b_{c\bar{c}}^2\pi}\Big)^{3/4}\exp\Big[-\frac{1}{2b_{c\bar{c}}^2}\Big(\vec{r}_{AB} + \frac{2m_l}{m_{123}}\vec{\xi}_2 - \frac{m_l}{m_{45}}\vec{\xi}_3\Big)^2\Big]$$
(18)

where $b_{c\bar{c}}^2 = \frac{2}{\omega m_c}$, $b_{p_1}^2 = \frac{2}{\omega m_\ell}$, and $b_{p_2}^2 = \frac{3}{2\omega m_\ell}$ are the harmonic oscillator width parameters of $c\bar{c}$ and proton systems, respectively, and

$$\exp(i\vec{k} \cdot \vec{r}_{A'B'}') = \exp\Big(\frac{i}{6}\vec{k} \cdot \Big[\vec{r}_{AB} - 2\frac{m_{15}}{m_{123}}\vec{\xi}_2 - \frac{m_{15}}{m_{45}}\vec{\xi}_3\Big]\Big),$$
(19)

describes the relative wave function between the final $c\bar{c}$ and proton, and $\exp(i\vec{\mathcal{P}} \cdot \vec{R}_{A'B'}')$ denotes the wave function of the CM motion with the coordinate of the CM motion $\vec{R}_{A'B'}' = \vec{R}_{AB}$ and the momentum of the five quark system $\mathcal{P}$ which obeys the momentum conservation rule $\vec{\mathcal{P}} = \vec{P}_{c\bar{c}} + \vec{P}_p = \vec{P}_{\Lambda_c} + \vec{P}_{\bar{D}}$.

The transition matrix element (TME) can be expressed as

$$\mathcal{M}_{fi} \equiv <f|\hat{P}_{34}\mathcal{H}_T|i>$$
$$= \int d^3r_1 d^3r_2 d^3r_3 d^3r_4 d^3r_5$$
$$\Big\{\Psi_{c\bar{c}}(\xi_3')\Psi_p(\xi_1', \xi_2')\frac{e^{i\vec{k} \cdot \vec{r}_{A'B'}'}}{\sqrt{V}}\frac{e^{i\vec{\mathcal{P}}_f \cdot \vec{R}_{A'B'}'}}{\sqrt{V}}\Big\}^\dagger \times \mathcal{H}_T.$$
$$\times \Big\{\sum_{i=1}^{10} c_i \mathcal{A} \int d\hat{S}_i \Pi_{k=1}^3 \psi_A(\vec{r}_k, \frac{\mu_{AB}}{M_A}\vec{S}_i)$$
$$\times \Pi_{l=4}^5 \psi_B(\vec{r}_l, -\frac{\mu_{AB}}{M_B}\vec{S}_i)Y_{LM}(\hat{S}_i)\tilde{\Phi}^{CSF}\Big\}.$$
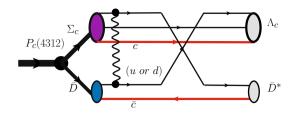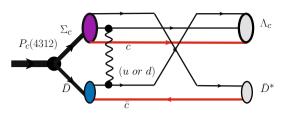(20)

Fig. 2 Schematic diagrams for the open charm decay $P_c(\Sigma_c + \bar{D}) \to \Lambda_c + \bar{D}^*$ with the quark re-arrangement between the 1-st and 4-th quarks. There are two types of interaction: One of them (left sub-diagram) is characterized by the interaction occurs between two quarks which participate in the quark-exchange at the same time. The other type (right sub-diagram) belongs to a type where only one interacting quark participates in the quark exchange at the same time, while the other interacting quark does not. It should be mentioned that in this process, there also exists another possible rearrangement which occurs between 2-nd and 4-th quarks

Table 1 The size parameters of final hadrons (in units of fm) with the universal $\omega = 0.45$ GeV and the quark mass of $m_l = 0.313$ GeV and $m_c = 1.54$ GeV

$b_{c\bar{c}}$	b_{p1}	b_{p2}	$b_{\bar{D}^*}$	$b_{\Lambda_c 1}$	$b_{\Lambda_c 2}$
$\sqrt{\dfrac{2}{\omega m_c}}$	$\sqrt{\dfrac{2}{\omega m_l}}$	$\sqrt{\dfrac{3}{2\omega m_l}}$	$\sqrt{\dfrac{m_l+m_c}{\omega m_l m_c}}$	$\sqrt{\dfrac{2}{\omega m_l}}$	$\sqrt{\dfrac{2m_l+m_c}{2\omega m_l m_c}}$
0.335	0.744	0.644	0.577	0.744	0.441

It should be mentioned that since what we would like to know, in this paper, is the decay behavior of P_c obtained with our model qualitatively, instead of doing lengthy detailed calculations on the transition matrix element, we make a rough estimate. Since TME is defined as the matrix element of the interactive Hamiltonian between two states and our bound state calculation of P_c shows that the main component of P_c is Σ_c-$\bar{D}$, in this work, we roughly assume that when the interactive Hamiltonian $\mathcal{H}_T$ brings the initial state P_c to an almost initial state, TME could be roughly approximated as a product of the averaged binding energy of P_c and the overlap between the initial and final states where the quark re-arrangement effect is included. In the practical calculation, we adopt the extended chiral constituent quark model with the quadratic confinement, which can better regenerate more existing data and give a more stable P_c-state binding energy. The resultant binding energy of P_c is about 10.3 MeV, and the range of binding energy in such a model is about $7-11$ MeV.

3.2 Open charm decay

On the other hand, it is said that the open-charm channel dominates the decay of P_c. Therefore, we should also calculate the partial decay width of such a channel. Here, we consider the quark re-arrangement effect of light quarks between the initial Σ_c and $\bar{D}$ hadrons. The detailed calculation for this mode is similar to the hidden charm decay except that the rearrangement here contains two possible rearrangements, $\hat{P}_{14}$ and $\hat{P}_{24}$. The schematic diagrams of this decay are shown in Fig. 2.

Similar to Eq. (7), the spin-isospin wave function of the final Λ_c and $\bar{D}^{(*)}$ states is given by

$$\Psi_{5q}^{(SF)} = \frac{1}{\sqrt{2}}\Big[\chi_\rho\xi_\rho + \chi_\lambda\xi_\lambda\Big]_{(SF)_{\Lambda_c}}^{(423(143))} \otimes \Big(q^{(1(2))}\bar{q}^{(5)}\Big)_{(SF)_{\bar{D}^{(*)}}},$$
(21)

where the superscript (423(or 143)) indicates that quarks in Λ_c are labeled by 4, 2, and 3 (or 1, 4, and 3), and (1(2)) and (5) denotes that quarks in $\bar{D}^{(*)}$ are marked by 1(or 2) and 5, respectively. The detailed forms of $\xi_{\rho,\lambda}$ (or $\chi_{\rho,\lambda}$) can also be found in Ref. [60].

3.3 Numerical results

The wave function of $P_c(4312)$ with a $\Sigma_c\bar{D}$ structure is solved in our previous bound state calculation [36]. In terms of this established wave function, the harmonic oscillator frequency ω is fixed as a universal value of 0.45 GeV. Then, the width parameter of the different hadrons in the final state can roughly be determined by the values of ω and different masses of quarks in corresponding hadrons, and are tabulated in Table 1. We first calculate the spin-flavor-color coefficients by using the spin-isospin wave functions in both initial and final states shown in Eqs. (7), (15) and (21) and recoupling coefficients. The obtained spin-flavor-color (SFC) coefficients are tabulated in Table 2.

Based on these width parameters, the final state wave functions written on the harmonic oscillator basis are entirely fixed. Then, we can calculate the decays widths.

Table 2 Color coefficient F^c and spin-flavor coefficient F^{SF} for $P_c(4312) \to p + J/\psi\,(\eta_c)$ and $P_c(4312) \to \Lambda_c + \bar{D}^{(*)}$, where $Dir.$, $\hat{P}_{41}$, $\hat{P}_{42}$, and $\hat{P}_{43}$ stand for the direct term, and permutations of (14), (24), and (34), respectively

| | $P_c(4312) \to p + J/\psi\,(\eta_c)$ | | | | $P_c(4312) \to \Lambda_c + \bar{D}^{(*)}$ | | | | | | | |
| | $p + J/\psi$ | | $p + \eta_c$ | | $\Lambda_c^{(423)} + \bar{D}^{(15)}$ | | $\Lambda_c^{(423)} + \bar{D}^{*(15)}$ | | $\Lambda_c^{(143)} + \bar{D}^{(25)}$ | | $\Lambda_c^{(143)} + \bar{D}^{*(25)}$ | |
	F^c	F^{SF}	F^c	F^{SF}	F^c	F^{SF}	F^c	F^{SF}	F^c	F^{SF}	F^c	F^{SF}
$Dir.$	$+\frac{1}{3}$	$+\frac{1}{2\sqrt{3}}$	$+\frac{1}{3}$	$\frac{1}{2}$	$+\frac{1}{3}$	0	$+\frac{1}{3}$	$-\frac{1}{2\sqrt{3}}$	$+\frac{1}{3}$	0	$+\frac{1}{3}$	$-\frac{1}{2\sqrt{3}}$
P_{14}	$-\frac{1}{3}$	$+\frac{1}{2\sqrt{3}}$	$-\frac{1}{3}$	$\frac{1}{2}$	$+1$	0	$+1$	0	$-\frac{1}{3}$	0	$-\frac{1}{3}$	$-\frac{1}{2\sqrt{3}}$
P_{24}	$-\frac{1}{3}$	$+\frac{1}{2\sqrt{3}}$	$-\frac{1}{3}$	$\frac{1}{2}$	$-\frac{1}{3}$	0	$-\frac{1}{3}$	$-\frac{1}{2\sqrt{3}}$	$+1$	0	$+1$	0
P_{34}	$+1$	0	$+1$	0	$-\frac{1}{3}$	0	$-\frac{1}{3}$	$+\frac{1}{2\sqrt{3}}$	$-\frac{1}{3}$	0	$-\frac{1}{3}$	$-\frac{1}{2\sqrt{3}}$

Table 3 The calculated partial decay widths (in units of MeV) comparing to the experimental measurement. The positive and negative deviations in the second line for $\Gamma_{J/\psi\,p}$, $\Gamma_{\eta_c\,p}$, $\Gamma_{\bar{D}^*\Lambda_c}$, and Γ_{Total} are based on about $+7\%$ and -32% uncertainties for the calculated binding energy of $P_c(4312)$ in the extended chiral constituent quark model

$\Gamma_{J/\psi p}$	$\Gamma_{\eta_c p}$	$\Gamma_{\bar{D}^*\Lambda_c}$	$\Gamma_{\bar{D}\Lambda_c}$	Γ_{Total}	$\Gamma_{Expt.}$
$0.033^{+0.005(14\%)}_{-0.018(54\%)}$	$0.066^{+0.009(14\%)}_{-0.035(54\%)}$	$6.16^{+0.87(14\%)}_{-3.31(54\%)}$	0	$6.25^{+0.88(14\%)}_{-3.36(54\%)}$	$9.8 \pm 2.7^{+3.5}_{-4.5}$

Working out the spatial integrals together with the SFC coefficients shown in Table 2, the partial decay widths can be calculated and are tabulated in Table 3.

It should be addressed that the spatial overlap between the initial and final states is model-dependent. However, the overlap in the spin-isospin and in color spaces between those states comes from the intrinsic properties of involved hadrons, including the quark re-arrangement, and therefore, is model-independent. In Table 2, it is shown that the spin-isospin factor in the $p\eta_c$ channel, where the re-arrangement effect is involved, is three times larger than that in the pJ/ψ channel. This is in agreement with the remarks in Ref. [21]. However, it is also shown in Table 3 that the ratio of the corresponding partial decay widths is not exactly 3, but around 2, although the same width parameter for both J/ψ and η_c in the final state has been taken. This is because that the overlap in the orbital space is closely related to the outgoing momentum k, namely it is momentum-dependent.

Moreover, our calculation shows that the partial decay width of the $(\Lambda_c \bar{D})$ channel vanishes. This is due to the zero overlap between the spin-isospin wave functions in the initial and final states where the quark re-arrangement involved (see Table 2). This outcome consists with the results from most other models in the molecular scenario on the hadronic degrees of freedom, where the t-channel pion-exchange between the pseudo-scalar meson $\bar{D}$ and Λ_c baryon does not exist. Finally, the result in Table 3 tells us that the decay channel $\Lambda_c \bar{D}^*$ is dominant and the branching ratios of the other two hidden charm decays are both less than 1%.

It is important to point out that the quark exchange effect comes from the Pauli principle (see Eq. (5)). Although the binding energy is small and the mass of $P_c(4312)$ is very close to the threshold of $\bar{D}\Sigma_c$, we still see that the effect of the quark exchange, from the last three terms on the right side of Eq. (5), plays a sizable role on the partial decays width of $P_c(4312)$. For example, such effect reduces the width of the $p J/\psi$ (or $p \eta_c$) decay from 0.163 MeV (or 0.313 MeV), which is solely contributed by the direct term (the first term on the right side of Eq. (5)), to 0.033 MeV (or 0.066 MeV), which is a sum of all the four terms on the right side of Eq. (5). For the open charm decays $\bar{D}^{(*)}\Lambda_c$, compared with the total contribution given by the sum of all the terms, the quark exchange effect also significantly reduces the width produced by the direct term by a factor of 0.74. Therefore, it is a defect that such an important re-arrangement effect cannot be accounted for in the calculations with the molecular scenario in the hadron level [16,18–20,22,31–33]. So far, how to make a direct connection between the calculations on the quark degrees of freedom and on the hadron degrees of freedom is still an open question. Moreover, one may also notice that the calculated branching ratios vary from tens of percentages [20] to even 0.03% [33] in the literature. It is necessary to pin down which one is more meaningful. Fortunately, our small $p J/\psi$ branching ratio is compatible with the upper limit of 4.6% given by the GlueX Collaboration [13], and the obtained total width of P_c of about 8.5 MeV is compatible with the data of $9.8 \pm 2.7^{+3.5}_{-4.5}$ MeV, although it is a rough estimate. Since our results are model-dependent in spatial integrals, different chiral constituent quark models may give different results. As shown in Ref. [36], the binding energy of P_c obtained from various constituent quark models, where they have different interactions and model parameter

sets, spreads in a large range of $9 - 42$ MeV. However, our calculation shows that by using the extended chiral constituent quark model with a quadratic confinement, one can better regenerate more existing experimental data and reproduce more stable binding energy of modeled P_c which compatible with the observation. Therefore, in this investigation, we adopt the extended chiral quark model with the quadratic confinement. In this particular interaction model, the maximal range of the binding energy of P_c is narrowed down to about $7 \sim 11$ MeV. For a reference, here, we only roughly estimate the deviation of the width caused by the deviation of the binding energy of P_c, $(10.3^{+0.7}_{-3.3}$ MeV), in this interaction model. The obtained uncertainties of the width are about $+14\%$ and -54%, respectively. We also put the deviations in Table 3. It shows that the obtained widths with deviations are still compatible with the experimental values with error. Of course, a more sophisticated calculation is urgent and necessary for finally identifying the structure of P_c. Now, we expect that by measuring the total width, especially the partial decay width of the open charm decays of $P_c(4312)$ such as $P_c(4312) \to \bar{D}^* \Lambda_c$ or $P_c(4312) \to \bar{D}\pi\Lambda_c$, more accurately, one may obtain the criterion for branching ratios and the applicability for different models.

4 Summary

In this work, we show a calculation for the selected strong decays of the newly observed $P_c(4312)$ with our chiral constituent quark model which has been proved to have the predictive power because most of existing data can be well-reproduced. The advantages of our calculation are twofold. (1) We are working in the quark level and the predicted mass of $P_c(4312)$ in our previous work is consistent with the observed data. (2) The wave function used in this calculation was obtained in the same calculation where the above mentioned mass is resulted without any additional parameters or form factors introduced by hands. Therefore, we expect that in comparison with other calculations, our model results are more meaningful. The branching ratios of the $p J/\psi$ and $p \eta_c$ decays in our model calculation are both less than 1%, and the latter is about 2 times larger than the former. In particular, the $\bar{D}^* \Lambda_c$ decay mode dominates. We also find that the quark exchange effect is sizeable. This is because that our $P_c(4312)$ wave function is on the quark degrees of freedom, where the effect of the quark re-arrangement can be considered explicitly. Therefore, in order to understand the nature of P_c, it is necessary to redo a calculation for the decays studied in this work in a more accurate way and predict more properties of P_c, such as the electromagnetic transition of $P_c(4312)$ as well as three-body decays, like $P_c(4312) \to \bar{D}^*\pi\Lambda_c$, for further experimental inspection. These studies are in progress.

Data Availability Statement This manuscript has associated data in a data repository. [Authors' comment: This is a theoretical study, the Hamiltonian of the system is a theoretical model and has been tested in our previous articles, for instance the reference [43] in our manuscript.]

Appendix

The unitary transformation between coordinate sets $(\vec{r}_1, \vec{r}_2, \vec{r}_3, \vec{r}_4, \vec{r}_5)$ and $(\vec{R}_{AB}, \vec{r}_{AB}, \vec{\xi}_1, \vec{\xi}_2, \vec{\xi}_3)$ in the initial state is

$$
\begin{pmatrix} \vec{r}_1 \\ \vec{r}_2 \\ \vec{r}_3 \\ \vec{r}_4 \\ \vec{r}_5 \end{pmatrix} = \begin{bmatrix} 1 & \frac{m_{45}}{m_{1-5}} & -\frac{m_2}{m_{12}} & -\frac{m_3}{m_{123}} & 0 \\ 1 & \frac{m_{45}}{m_{1-5}} & +\frac{m_1}{m_{12}} & -\frac{m_3}{m_{123}} & 0 \\ 1 & \frac{m_{45}}{m_{1-5}} & 0 & +\frac{m_{12}}{m_{123}} & 0 \\ 1 & -\frac{m_{123}}{m_{1-5}} & 0 & 0 & -\frac{m_5}{m_{45}} \\ 1 & -\frac{m_{123}}{m_{1-5}} & 0 & 0 & +\frac{m_4}{m_{45}} \end{bmatrix} \begin{pmatrix} \vec{R}_{AB} \\ \vec{r}_{AB} \\ \vec{\xi}_1 \\ \vec{\xi}_2 \\ \vec{\xi}_3 \end{pmatrix},
$$

(22)

and the unitary transformation between coordinate sets $(\vec{r}_1, \vec{r}_2, \vec{r}_3, \vec{r}_4, \vec{r}_5)$ and $(\vec{R}'_{A'B'}, \vec{r}'_{A'B'}, \vec{\xi}'_1, \vec{\xi}'_2, \vec{\xi}'_3)$ in the final state is

$$
\begin{pmatrix} \vec{R}'_{A'B'} \\ \vec{r}'_{A'B'} \\ \vec{\xi}'_1 \\ \vec{\xi}'_2 \\ \vec{\xi}'_3 \end{pmatrix} = \begin{bmatrix} \frac{m_1}{m_{1-5}} & \frac{m_2}{m_{1-5}} & \frac{m_4}{m_{1-5}} & \frac{m_3}{m_{1-5}} & \frac{m_5}{m_{1-5}} \\ \frac{m_1}{m_{1-5}} & \frac{m_2}{m_{1-5}} & \frac{m_4}{m_{1-5}} & -\frac{m_3}{m_{1-5}} & -\frac{m_5}{m_{1-5}} \\ -1 & +1 & 0 & 0 & 0 \\ -\frac{m_1}{m_{12}} & -\frac{m_2}{m_{12}} & +1 & 0 & 0 \\ 0 & 0 & 0 & -1 & +1 \end{bmatrix} \begin{pmatrix} \vec{r}_1 \\ \vec{r}_2 \\ \vec{r}_4 \\ \vec{r}_3 \\ \vec{r}_5 \end{pmatrix}.
$$

(23)

References

1. H.X. Chen, W. Chen, X. Liu, S.L. Zhu, Phys. Rept. **639**, 1 (2016)

2. F.K. Guo, C. Hanhart, U.G. Meissner, Q. Wang, Q. Zhao, B.S. Zou, Rev. Mod. Phys. **90**, 015004 (2018)
3. A. Esposito, A. Pilloni, A.D. Polosa, Phys. Rept. **668**, 1 (2017)
4. M. Karliner, J.L. Rosner, T. Skwarnicki, Ann. Rev. Nucl. Part. Sci. **68**, 17 (2018)
5. Y. Dong, A. Faessler, V.E. Lyubovitskij, Prog. Part. Nucl. Phys. **94**, 282 (2017)
6. Y.R. Liu, H.X. Chen, W. Chen, X. Liu, S.L. Zhu, Prog. Part. Nucl. Phys. **107**, 237 (2019)
7. L. Maiani, F. Piccinini, A.D. Polosa, V. Riquer, Phys. Rev. D **71**, 014028 (2005)
8. L. Maiani, V. Riquer, F. Piccinini, A.D. Polosa, Phys. Rev. D **72**, 031502 (2005)
9. L. Maiani, F. Piccinini, A.D. Polosa, V. Riquer, Phys. Rev. D **89**, 114010 (2014)
10. F. K. Guo, X. H. Liu, S. Sakai, "Threshold cusps and triangle singularities in hadronic reactions," arXiv:1912.07030 [hep-ph]
11. S.L. Olsen, T. Skwarnicki, D. Zieminska, Rev. Mod. Phys. **90**(1), 015003 (2018)
12. N. Brambilla, S. Eidelman, C. Hanhart, A. Nefediev, C.P. Shen, C.E. Thomas, A. Vairo, C.Z. Yuan,. arXiv:1907.07583 [hep-ex]
13. A. Ali *et al.* [GlueX Collaboration], Phys. Rev. Lett. **123**,(7) 072001 (2019)
14. R. Aaij et al., LHCb Collaboration. Phys. Rev. Lett. **115**, 072001 (2015)
15. R. Aaij *et al.* [LHCb Collaboration], Phys. Rev. Lett. **122**(22), 222001 (2019)
16. C.J. Xiao, Y. Huang, Y.B. Dong, L.S. Geng, D.Y. Chen, Phys. Rev. D **100**(1), 014022 (2019)
17. R. Chen, Z.F. Sun, X. Liu, S.L. Zhu, Phys. Rev. D **100**(1), 011502 (2019)
18. J. He, D.Y. Chen, Eur. Phys. J. C **79**(11), 887 (2019)
19. X.Y. Wang, X.R. Chen, J. He, Phys. Rev. D **99**(11), 114007 (2019)
20. T. Gutsche, V.E. Lyubovitskij, Phys. Rev. D **100**(9), 094031 (2019)
21. M.B. Voloshin, Phys. Rev. D **100**(3), 034020 (2019)
22. Y.H. Lin, B.S. Zou, Phys. Rev. D **100**(5), 056005 (2019)
23. G.J. Wang, L.Y. Xiao, R. Chen, X.H. Liu, X. Liu, S.L. Zhu,. arXiv:1911.09613 [hep-ph]
24. L. Meng, B. Wang, G.J. Wang, S.L. Zhu, Phys. Rev. D **100**(1), 014031 (2019)
25. X.Z. Weng, X.L. Chen, W.Z. Deng, S.L. Zhu, Phys. Rev. D **100**(1), 016014 (2019)
26. C. Fernndez-Ramrez *et al.* [JPAC Collaboration], Phys. Rev. Lett. **123**(9) (2019), 092001
27. H.X. Chen, W. Chen, X. Liu, T.G. Steele, S.L. Zhu, Phys. Rev. Lett. **115**(17), 172001 (2015)
28. R. Chen, X. Liu, X.Q. Li, S.L. Zhu, Phys. Rev. Lett. **115**(13), 132002 (2015)
29. X.H. Liu, M. Oka, Q. Zhao, Phys. Lett. B **753**, 297 (2016)
30. S. Takeuchi, M. Takizawa, Phys. Lett. B **764**, 254 (2017)
31. Y. Yamaguchi, E. Santopinto, Phys. Rev. D **96**(1), 014018 (2017)
32. Q.F. Lyu, Y.B. Dong, Phys. Rev. D **93**(7), 074020 (2016)
33. Y.H. Lin, C.W. Shen, F.K. Guo, B.S. Zou, Phys. Rev. D **95**(11), 114017 (2017)
34. J.J. Wu, R. Molina, E. Oset, B.S. Zou, Phys. Rev. Lett. **105**, 232001 (2010)
35. J.J. Wu, R. Molina, E. Oset, B.S. Zou, Phys. Rev. C **84**, 015202 (2011)
36. W.L. Wang, F. Huang, Z.Y. Zhang, B.S. Zou, Phys. Rev. C **84**, 015203 (2011)
37. Z.C. Yang, Z.F. Sun, J. He, X. Liu, S.L. Zhu, Chin. Phys. C **36**, 6 (2012)
38. Yuan Xiuqiang, Yu. Zhang Zongye, Shen Pengnian Youwen, High Energy Phys. Nucl. Phys. **22**, 718 (1998)
39. P.N. Shen, Z.Y. Zhang, Y.W. Yu, X.Q. Yuan, S. Yang, J. Phys. G **25**, 1807 (1999)
40. Q.B. Li, P.N. Shen, Eur. Phys. J. A **8**, 417 (2000)
41. Q.B. Li, P.N. Shen, Z.Y. Zhang, Y.W. Yu, Nucl. Phys. A **683**, 487 (2001)
42. P.N. Shen, Q.B. Li, Z.Y. Zhang, Y.W. Yu, Nucl. Phys. A **675**, 234 (2000)
43. X.Q. Yuan, Z.Y. Zhang, Y.W. Yu, P.N. Shen, Phys. Rev. C **60**, 045203 (1999)
44. M. Bashkanov et al., Phys. Rev. Lett. **102**, 052301 (2009)
45. P. Adlarson et al., WASA-at-COSY Collaboration. Phys. Rev. Lett. **106**, 242302 (2011)
46. P. Adlarson et al., WASA-at-COSY Collaboration. Phys. Lett. B **721**, 229 (2013)
47. P. Adlarson *et al.* [WASA-at-COSY Collaboration], Phys. Rev. Lett. **112**(20), 202301 (2014)
48. H. Clement, Prog. Part. Nucl. Phys. **93**, 195 (2017)
49. Y. Dong, P. Shen, F. Huang, Z. Zhang, Phys. Rev. C **91**(6), 064002 (2015)
50. Y. Dong, F. Huang, P. Shen, Z. Zhang, Phys. Rev. C **94**(1), 014003 (2016)
51. Y. Dong, F. Huang, P. Shen, Z. Zhang, Chin. Phys. C **41**(10), 101001 (2017)
52. Y. Dong, F. Huang, P. Shen, Z. Zhang, Phys. Lett. B **769**, 223 (2017)
53. Y. Dong, P. Shen, F. Huang, Z. Zhang, Int. J. Mod. Phys. A **33**(33), 1830031 (2018)
54. Y. Dong, F. Huang, P. Shen, Z. Zhang, Phys. Rev. D **96**(9), 094001 (2017)
55. Y. Dong, P. Shen, Z. Zhang, Phys. Rev. D **97**(11), 114002 (2018)
56. Y. Dong, P. Shen, Z. Zhang, Int. J. Mod. Phys. A **34**(18), 1950100 (2019)
57. M. Bashkanov, Stanley J. Brodsky, H. Clement, Phys. Lett. **727**, 438 (2013)
58. F. Huang, Z.Y. Zhang, P.N. Shen, W.L. Wang, Chin. Phys. C **39**(7), 071001 (2015)
59. F. Huang, P.N. Shen, Y.B. Dong, Z.Y. Zhang, Sci. China Phys. Mech. Astron. **59**(2), 622002 (2016)
60. F.E. Close, *An introduction to quarks and partons* (Academic Press, 1979)
61. T. Barnes, N. Black, E.S. Swanson, Phys. Rev. C **63**, 025204 (2001)
62. Y.Q. Li, X.M. Xu, Nucl. Phys. A **794**, 210 (2007)
63. K. Yang, X.M. Xu, H.J. Weber, Phys. Rev. D **96**(11), 114025 (2017)
64. M. Maruyama, T. Ueda, Nucl. Phys. A **364**, 297 (1981)
65. S. Furui, A. Faessler, S.B. Khadkikar, Nucl. Phys. A **424**, 495 (1984)
66. A.M. Green, J.A. Niskanen, Nucl. Phys. A **430**, 605 (1984)